2004 International Symposium on Nonlinear
Theory and its Applications (NOLTA2004)
Fukuoka, Japan, Nov. 29 - Dec. 3, 2004

A Challenge to Bernstein's Degrees-of-Freedom Problem in Both Cases of Human and Robotic Multi-Joint Movements

Suguru Arimoto†

†Department of Robotics, Ritsumeikan University
1-1-1 Nojihigashi, Kusatsu, Shiga, 525-8577 Japan
Email: arimoto@se.ritsumei.ac.jp

Abstract—This paper aims at challenging Bernstein's problem called the "Degrees-of-Freedom problem", which is known to remain unsolved from both the physiological and robotics viewpoints. More than a half century ago A.N. Bernstein observed and claimed that "dexterity" resident in human limb motion emerges from accumulated involvement of multi-joint movements in surplus DOF. It is also said in robotics that redundancy of DOFs in robot mechanisms may contribute to enhancement of dexterity and versatility. However, kinematic redundancy incurs a problem of ill-posedness of inverse kinematics from task-description space to joint space. In the history of robotics research such ill-posedness problem of inverse-kinematics has not yet been attacked directly but circumvented by introducing an artificial performance index and determining uniquely an inverse kinematics solution by minimizing it. Instead of it, this paper introduces two novel concepts named "stability on a manifold" and "transferability to a submanifold" in treating the case of human multi-joint movements of reaching and shows that a sensory feedback from task space to joint space together with a set of adequate dampings (joint velocity feedbacks) enables any solution to the overall closed-loop dynamics to converge naturally and coordinately to a lower-dimensional manifold describing a set of joint states fulfilling a given motion task. This means that, without considering any type of inverse kinematics, the reaching task can be accomplished by a sensory feedback with adequate choices of a stiffness parameter and damping coefficients. It is also shown that these novel concepts can cope with annoying characteristics called "variability" of redundant joint motions seen typically in human skilled reaching. Finally, it is pointed out that the proposed control signals can be generated in a feedforward manner in case of human limb movements by referring to mechano-chemical characteristics of activation of muscles. Based on this observation, generation of a human skilled movement can be interpreted in terms of the proposed "Virtual-Spring"hypothes instead of the traditional "Equilibrium-point" hypothesis.

1. Introduction

This paper is concerned with a challenge to one of unsolved problems posed by A.N. Bernstein [1] [2] as the Degrees-of-Freedom problem, particularly, in case of human or robotic multi-joint movements of reaching as shown in Fig.1. The problem is how to generate a joint motion so as to transfer the endpoint of an upper limb with four joints (shoulder, elbow, wrist, and finger MP joint) to a given target point $\boldsymbol{x}_d = (x_d, y_d)$ in the two-dimensional horizontal plane. Since the objective task $\boldsymbol{x}_d$ is given in the task space $\boldsymbol{x} \in X(= R^2)$ and the joint coordinates $q = (q_1, q_2, q_3, q_4)^{\mathrm{T}}$ are of four-dimension, there exists an infinite number of inverses q_d that realize $\boldsymbol{x}(q_d) = \boldsymbol{x}_d$ and hence the problem of obtaining inverse kinematics from the task description space X to the 4-dimensional joint space becomes ill-posed. Under this circumstances, however, it is necessary to generate joint motions $q(t)$ starting from a given initial point $\boldsymbol{x}(0) = (x(0), y(0))$ in X with some initial posture $q(0) = (q_1(0), \cdots, q_4(0))^{\mathrm{T}}$ and leading the endpoint trajectory $\boldsymbol{x}(t)$ to reach the target $\boldsymbol{x}_d$ as $t \to \infty$. In order to get rid of such ill-posedness, many methods have been proposed as surveyed in a special issue of the journal [3] and a book specially dedicated to problems of redundancy [4]. Most of them are based on an idea of introducing some extra and artificial performance index for determining uniquely an appropriate joint space trajectory by minimizing it. In fact, examples of such performance index in robotics research are the followings: kinetic energy [5], quadratic norm of joint control torque [6], manipulability index [7], virtual fatigue function [8], etc. [9] [10]. Most of proposed methods have been explicitly or implicitly based on the Jacobian pseudoinverse approach for planning an optimized joint velocity trajectory $\dot{q}(t)$ together with an extra term $(I - J^{+}(q)J(q))\boldsymbol{v}$, where $\boldsymbol{v}$ is determined by optimizing

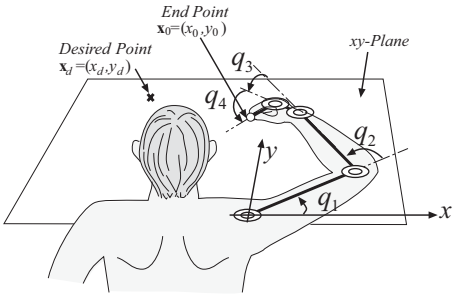

Figure 1: "Reaching" by means of a surplus DOF system of hand-arm dynamics.

the performance index, $J(q)$ stands for the Jacobian matrix of task coordinates $\boldsymbol{x}$ in joint coordinates q, and $J^+(q)$ the pseudoinverse of $J(q)$. In the history of robot control the idea of use of the pseudoinverse for generation of joint trajectories for redundant robots was initiated by Whitney [11] and analyzed more in details by Liegeois [12]. However, it is impossible to calculate $J^+(q_d)$ in advance because q_d is undetermined. Therefore, it is recommended that a control signal u to be exerted through joint actuators of the robot is designed as

$$u = -C\dot{q} + J^{\mathrm{T}}(q)K(\boldsymbol{x}(q) - \boldsymbol{x}_d) + \{I - J^+(q)J(q)\}\boldsymbol{v} \qquad (1)$$

where C stands for a constant positive definite matrix for damping shaping and K a constant definite positive definite gain matrix. On the other hand, there is the vast literature of research works concerned with even a simple multi-joint reaching motion or pointing movement in physiology, which are, for example, Feldman [13], Flash [14], Flash and Hogan [15], Georgopoulos [16], and Bizzi et al [17]. Most of them published in physiological journals are more or less affected by the equilibrium point (EP) hypothesis of motor control found by Feldman [18] and observed by Bizzi et al. [19] as spring-like motion of a group of muscles. This EP hypothesis can be interpreted in the control-theoretic language such that for a specified arm endpoint $\boldsymbol{x}_d$ in cartesian space the central part of control for reaching it must be composed of the term $J^{\mathrm{T}}(q)K(\boldsymbol{x} - \boldsymbol{x}_d)$ which corresponds to assuming introduction of an artificial potential $\Delta\boldsymbol{x}^{\mathrm{T}}K\Delta\boldsymbol{x}/2$ in the external world (task space), where $\Delta\boldsymbol{x} = \boldsymbol{x} - \boldsymbol{x}_d$. This idea is also known in robotics as the PD feedback with damping shaping first proposed by Takegaki and Arimoto[20]. In the case of redundant multi-joint reaching, however, there arises the same problem of ill-posedness of inverse kinematics. Thus, in parallel with the vast literature [3–12] in robotics research, many methods for elimination of redundancy of DOFs have been proposed in the physiological literature initiated by Hogan [21]. Most of them are samely based on introduction of extra performance criterion to be optimized, which are in the following: squared norm of joint jerks (rate of change of acceleration) [21][15], energy [22], effort applied during movement [23], minimum-torque [24], and minimum torque-change [25] and some other cost functions [26] though some of them are not used for redundancy resolution. Nevertheless, even all performance indices that lead successfully to unique determination of the inverse kinematics are not well-grounded physiologically and none of physiological evidence or principle that associates such a performance index to generation of human movements could be found.

In this paper, we resolve this ill-posedness of inverse kinematics without considering any kind of inverse problems and without introducing any type of artificial performance index for the multi-joint reaching problem posed above. Instead, we use a surprisingly simpler sensory feedback scheme described as

$$u = -C\dot{q} - J^{\mathrm{T}}(q)k\Delta\boldsymbol{x} \qquad (2)$$

where $\Delta\boldsymbol{x} = \boldsymbol{x} - \boldsymbol{x}_d$, k a single stiffness parameter. This means that the control signal is composed of only two terms, one is a damping term (angular velocity feedback) and the other is a sensory feedback from task space with the stiffness parameter k modified by the transpose of Jacobian $J(q)$. This is nothing else but a task-space PD feedback scheme with damping shaping in the case of control of non-redundant robot manipulators [27]. It is proved theoretically that adequate choices of gain matrices C and stiffness parameter k render the closed-loop system dynamics convergent as time elapses, that is, $\boldsymbol{x}(t) \to \boldsymbol{x}_d$ and $\dot{q}(t) \to 0$ as $t \to \infty$. However, owing to the joint redundancy, the convergence in task space does not directly imply the convergence of joint variables $q(t)$ to some posture. In the paper, by introducing a novel concept named "stability on a manifold" it is shown that $q(t)$ remains in a specified region in joint space such that the Jacobian matrix is nondegenerated and there does not arise any unexpected self-motion inherent to redundant systems. In other words, the control scheme of eq.(2) suggests that the problem of elimination of joint redundancy need not be solved but can be ignored in control of the dynamics. Or it can be said that a natural physical principle for economies of skilled motions like the principle of least action in Newtonian mechanics may work in elimination of redundancy. Another concept named "transferability to a submanifold" is also introduced for discussing the asymptotic convergence in a case of middle-range reaching. These two concepts were originally and very recently defined in cases of control of multi-fingered hands with joint redundancy and control of a hand-writing robot with surplus DOFs [28][29].

All the simulation results conducted on the basis of the closed-loop dynamics obtained by substituting the control signal of eq.(2) into the Lagrange equation of motion seem to support the EP-hypothesis. However, the hypothesis has recently been re-considered in a more soplisticated manner by Won & Hogan [30] in order to take into account the phenomenon of relatively low stiffness of spring-like forces during limb movements observed by Bennet et al. [31] and Gomi et al. [32]. The final section dedicates itself to the argument that, instead of the EP-hypothesis, the Virtual-Spring hypothesis is well capable to interpret how a skilled motion with redundant DOFs can be generated irrespective of low or high stiffness of individual muscle contraction forces. Further, based on the Virtual-spring hypothesis together with referring to chemical characteristics of activation of muscles, generation of task-space sensory feedback signals can be interpreted as a time-varying potential signal that can exert at joints in a feedforward manner. Finally, it is shown from computer simulation results that a robotic reaching motion with redundant DOFs exhibiting all typical characteristics of human skilled multi-joint reaching as Latash pointed out [33] can be realized by such a simple control signal.

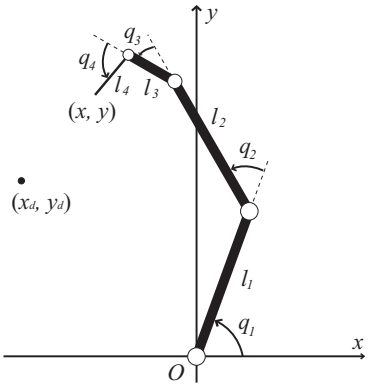

Figure 2: Initial posture of the arm-hand system with four joints. The point (x_d, y_d) denotes the target for the robot endpoint.

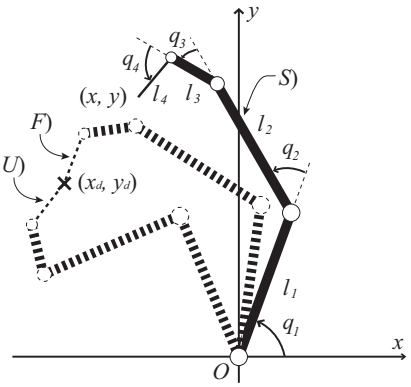

Figure 3: S) Starting posture, F) Final posture, U) Unreasonable posture

2. Closed-loop Dynamics of Multi-joint Reaching Movement

Lagrange's equation of motion of a multi-joint system whose motion is confined to a plane as shown in Fig.1 is described by the formula (see [34])

$$H(q)\ddot{q} + \left\{\frac{1}{2}\dot{H}(q) + S(q,\dot{q})\right\}\dot{q} = u \tag{3}$$

where $q = (q_1, q_2, q_3, q_4)^{\mathrm{T}}$ denotes the vector of joint angles, $H(q)$ the inertia matrix, and $S(q, \dot{q})\dot{q}$ the gyroscopic force term including centrifugal and Coriolis force. It is well known that the iniertia matrix $H(q)$ is symmetric and positive definite and there exist a positive constant h_m together with a positive definite constant diagonal matrix H_0 such that

$$h_m H_0 \le H(q) \le H_0 \tag{4}$$

for any q. It should be also noted that $S(q, \dot{q})$ is skew symmetric and linear and homogeneous in $\dot{q}$. Any entry of $H(q)$ and $S(q, \dot{q})$ is constant or a sinusoidal function of components of q.

For a given specified target position $\boldsymbol{x}_d = (x_d, y_d)$ as shown in Fig.1, if the control input of eq.(2) is used at joint actuators then the closed-loop equation of motion of the system can be expressed as

$$H(q)\ddot{q} + \left\{\frac{1}{2}\dot{H}(q) + S(q,\dot{q}) + C\right\}\dot{q} + J^{\mathrm{T}}(q)k\Delta\boldsymbol{x} = 0 \tag{5}$$

which follows from substitution of eq.(2) into eq.(3). Since $\dot{\boldsymbol{x}} = J(q)\dot{q}$, the inner product of eq.(5) with $\dot{q}$ is reduced to

$$\frac{\mathrm{d}}{\mathrm{d}t}E = -\dot{q}^{\mathrm{T}}C\dot{q} \tag{6}$$

where E stands for the total energy, i.e.,

$$E(q,\dot{q}) = \frac{1}{2}\dot{q}^{\mathrm{T}}H(q)\dot{q} + \frac{k}{2}\Delta\boldsymbol{x}^{\mathrm{T}}\Delta\boldsymbol{x} \tag{7}$$

Evidently the first term of this quantity E stands for the kinetic energy of the system. The second term is called an artificial potential in this paper that appears due to addition of equilibrium point control $J^{\mathrm{T}}(q)k\Delta\boldsymbol{x}$ based on the error $\Delta\boldsymbol{x}$ expressed in cartesian space. As it is well known in robot control (see [34]), the relation of eq.(6) denotes passivity of the closed-loop dynamics of eq.(5). It also reminds us of Lyapunov's stability analysis, since it shows that the derivative of a scalar function E in time t is negative semi-definite. However, it should be noted that the scalar function $E(q, \dot{q})$ is not positive definite with respect to the state vector $(q, \dot{q}) \in R^8$. In fact, E includes only a quadrative term of two-dimensional vector $\Delta\boldsymbol{x}$ except the kinetic energy as a positive definite quadratic function of $\dot{q}$. Therefore, it is natural and reasonable to introduce a manifold of 2-dimension defined as

$$M_2 = \{(q,\dot{q}) : E(q,\dot{q}) = 0\ (\dot{q} = 0, \boldsymbol{x}(q) = \boldsymbol{x}_d)\}$$

which is called the zero space in the literature of robotics research (for example, [6]). Next, consider a posture $(q^0, 0)$ with still state (i.e., $\dot{q} = 0$) whose endpoint is located at $\boldsymbol{x}_d$, i.e., $\boldsymbol{x}(q^0) = \boldsymbol{x}_d$ and hence $(q^0, 0) \in M_2$, and analyze stability of motion of the closed-loop dynamics in a neighborhood of this equilibrium state. This equilibrium state in R^8 is called in this paper the reference equilibrium state.

It is now necessary to introduce the concept of neighborhoods of the reference equilibrium state $(q^0, 0) \in M_2$ in R^8, which are conveniently defined with positive parameters $\delta > 0$ and $r_0 > 0$ as

$$N^8(\delta, r_0) = \left\{(q,\dot{q}) : E(q,\dot{q}) \le \delta^2 \quad \text{and} \quad \|q - q^0\|_K \le r_0\right\}$$

where $\|q - q^0\|_K = \left\{\frac{1}{2}(q - q^0)^{\mathrm{T}}H(q)(q - q^0)\right\}^{1/2}$ (see Fig.4). The necessity of imposing the inequality condition $\|q - q^0\|_K \le r_0$ comes from avoiding arise of possible movements such as self-motion [32] due to redundancy of DOFs far from the original posture. In fact, for the given endpoint $\boldsymbol{x}_d$ with the reference state as shown by the mark F)

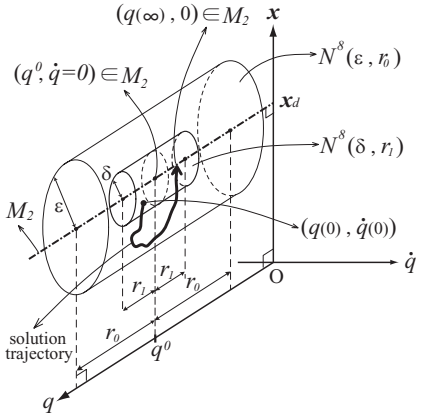

Figure 4: Definitions of "stability on a manifold" and "transferability to a submanifold".

in Fig.3, one possible state with the posture marked by S) in Fig.3 may be inside $N^8(\delta, r_0)$ but another state marked by U) must be excluded from the neighborhood $N^8(\delta, r_0)$ by choosing $r_0 > 0$ appropriately, because the overall posture of U) is by far deviated from that of the original reference equilibrium state $(q^0, 0)$. Further, it is necessary to assume that the reference equilibrium state $(q^0, 0)$ is considerably distant from the posture that has singularity of Jacobian matrix $J(q)$, which happens if and only if $q_2 = q_3 = q_4 = 0$.

We are now in a position to define the concept of stability of the reference equilibrium state lying on the manifold M_2.

Definition 1 If for an arbitrarily given $\varepsilon > 0$ there exist a constant $\delta > 0$ depending on ε and another constant $r_1 > 0$ independent of ε and less than r_0 such that a solution trajectory $(q(t), \dot{q}(t))$ of the closed-loop dynamics of eq.(5) starting from any initial state $(q(0), \dot{q}(0))$ inside $N^8(\delta(\varepsilon), r_1)$ remains in $N^8(\varepsilon, r_0)$, then the reference equilibrium state $(q^0, 0)$ is called stable on a manifold (see Fig.4).

Definition 2 If for a reference equilibrium state $(q^0, 0) \in R^8$ there exist constants $\varepsilon_1 > 0$ and $r_1 > 0$ $(r_1 < r_0)$ such that any solution of the closed-loop dynamics of eq.(5) starting from an arbitrary initial state in $N^8(\varepsilon_1, r_1)$ remains in $N^8(\varepsilon_1, r_0)$ and converges asymptotically as $t \to \infty$ to some point on $M_2 \cap N^8(\varepsilon_1, r_0)$, then the neighborhood $N^8(\varepsilon_1, r_1)$ of the reference equilibrium state $(q^0, 0)$ is said to be transferable to a submanifold of M_2.

This definition means that, even if a still state $(q^0, 0) \in M_2$ of the multi-joint system is forced to move instantly to a different state $(q(0), \dot{q}(0))$ in a neighborhood of $(q^0, 0)$ by being exerted from some external disturbance, the sensory feedback control of eq.(2) assures that the system's state soon recovers to another still state $(q^\infty, 0) \in M_2 \cap N^8(\varepsilon_1, r_0)$ whose endpoint attains at the original point $\boldsymbol{x}(q^\infty) = \boldsymbol{x}_d$ though the convergent posture q^∞ possibly differs from the original one q^0 but remains within $\|q^\infty - q^0\|_K \leq r_0$.

Table 1: Lengths of upper arm (l_1), lower arm (l_2), palm (l_3), and index finger (l_4) together with corresponding masses (m_i, $i = 1, \cdots, 4$) and inertia moments (I_i, $i = 1, \cdots, 4$). The data are taken from an average male adult.

arm	link1 length	l_1	0.2800	[m]
	link2 length	l_2	0.2800	[m]
	link3 length	l_3	0.09500	[m]
	link4 length	l_4	0.09000	[m]
	link1 cylinder radius	r_1	0.04000	[m]
	link2 cylinder radius	r_2	0.03500	[m]
	link3 cuboid height	h_3	0.08500	[m]
	link3 cuboid depth	d_3	0.03000	[m]
	link4 cylinder radius	r_4	0.009500	[m]
	link1 mass	m_1	1.407	[kg]
	link2 mass	m_2	1.078	[kg]
	link3 mass	m_3	0.2423	[kg]
	link4 mass	m_4	0.02552	[kg]
	link1 inertia moment	I_1	9.758×10^{-3}	[kgm^2]
	link2 inertia moment	I_2	7.370×10^{-3}	[kgm^2]
	link3 inertia moment	I_3	2.004×10^{-4}	[kgm^2]
	link4 inertia moment	I_4	1.780×10^{-5}	[kgm^2]

Table 2: Initial conditions.

$q_1(0)$	83.00	[deg]
$q_2(0)$	45.00	[deg]
$q_3(0)$	40.00	[deg]
$q_4(0)$	74.00	[deg]
$x(0)$	-0.2734	[m]
$y(0)$	0.4788	[m]
$\|\Delta \boldsymbol{x}\|_2$	0.1173	[m]

Table 3: Numerical values of inertia matrix $H(q(t))$ at $t = 0$ with the posture expressed in Fig.3 (a).

$$H(q(0)) = \begin{bmatrix} 2.886 \times 10^{-1} & 1.011 \times 10^{-1} & 4.004 \times 10^{-3} & -3.314 \times 10^{-4} \\ 1.011 \times 10^{-1} & 5.630 \times 10^{-2} & 3.964 \times 10^{-3} & -3.123 \times 10^{-5} \\ 4.004 \times 10^{-3} & 3.964 \times 10^{-3} & 1.107 \times 10^{-3} & 9.954 \times 10^{-5} \\ -3.314 \times 10^{-4} & -3.123 \times 10^{-5} & 9.954 \times 10^{-5} & 6.947 \times 10^{-5} \end{bmatrix}$$

3. Short-range Reaching

According to the energy balance law expressed by eq.(6), the total energy $E(t)(= E(q(t)), \dot{q}(t))$ is decreasing with increasing t as far as $\dot{q} \neq 0$ for an arbitrary positive definite damping gain matrix C. However, the motion profile $\boldsymbol{x}(t)$ of the endpoint is quite sensitive to choice for $c_i > 0$ for $i = 1, \cdots, 4$ where $C = \mathrm{diag}(c_1, \cdots, c_4)$ though for a broad

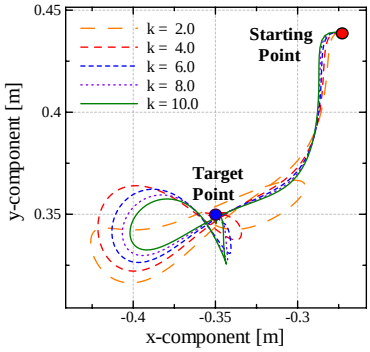

Figure 5: Endpoint trajectories of multi-joint reaching movements when damping factors of eq.(8) is used.

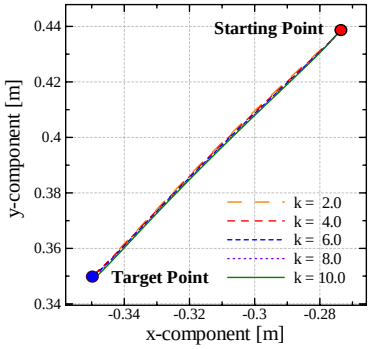

Figure 6: Endpoint trajectories of reaching movements when damping factors of eq.(9) is used.

range of choice for c_i $(i = 1, \cdots, 4)$ the endpoint $\boldsymbol{x}(t)$ eventually converges to the target if the stiffness k is chosen adequately. For example, we show several endpoint trajectories for different k in Fig.5 obtained by computer simulation based on a human model shown in Table 1 in the case that the initial point $\boldsymbol{x}(0)$ in task space $X(= R^2)$ and its corresponding initial posture $q(0)$ are set as in Table 2, where damping gains are chosen as

$$c_1 = c_2 = c_3 = c_4 = 0.003 \quad [\text{Ns}] \tag{8}$$

The endpoint trajectory $\boldsymbol{x}(t)$ starting from the initial posture shown as S) in Fig.3 is going to approach the target but overruns and oscillates around the target $\boldsymbol{x}_d$, but in a long run it converges to the target and stops with the final posture shown as U) in Fig.3 when $k = 8.0$ is chosen.

According to Latash [33], human skilled multi-joint reaching is characterized as follows:

a) The profile of the endpoint trajectory in task space X becomes a quasi-straight line,

b) the velocity profile of it in X becomes symmetric and bell-shaped,

c) the acceleration profile has double peaks,

d) but each profile of time histories of joint angles $q_i(t)$ and angular velocities $\dot{q}_i(t)$ may differ for $i = 1, 2, \cdots, 4$.

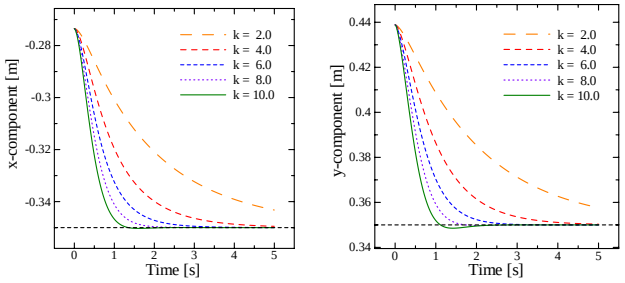

(a) $x(t)$ (b) $y(t)$

Figure 7: Transient responses of x and y when damping factors of eq.(9) are chosen.

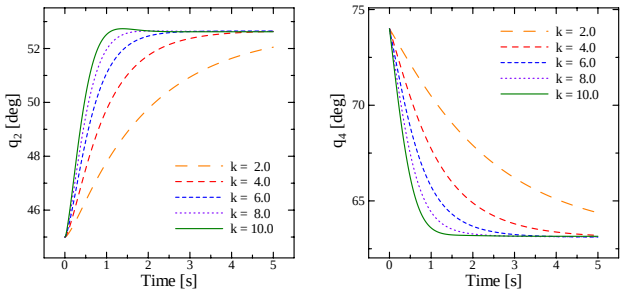

(a) $q_2(t)$ (b) $q_4(t)$

Figure 8: Transient responses of joint angles q_2 and q_4 when damping factors of eq.(9) are chosen.

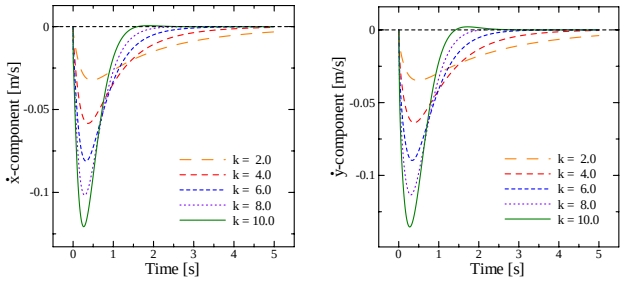

(a) $\dot{x}(t) = \mathrm{d}x(t)/\mathrm{d}t$ (b) $\dot{y}(t) = \mathrm{d}y(t)/\mathrm{d}t$

Figure 9: Transient responses of velocities $\dot{x}$ and $\dot{y}$ when damping factors of eq.(9) are chosen.

We are now in a position to answer to the question whether it is possible to find a set of adequate damping factors c_i $(i = 1, \cdots, 4)$ together with an adequate stiffness parameter $k > 0$ so that the simpler sensory feedback of eq.(2) leads to the skilled motion of reaching realizing an approximately rectilinear endpoint trajectory without incurring any noteworthy self-motion. We select damping factors as fallows:

$$c_1 = 1.89, \quad c_2 = 1.21, \quad c_3 = 0.29, \quad c_4 = 0.070 \tag{9}$$

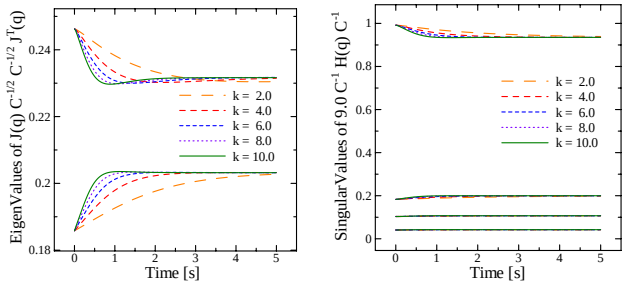

(a) (b)

Figure 10: Transient eigenvalues of 2×2 matrix $J(q)C^{-1}J^{\mathrm{T}}(q)$ (left) and 4×4 matrix $9.0C^{-1}H(q)C^{-1}$ (right).

Then, numerical solutions of the closed-loop dynamics of eq.(5) for different stiffness parameters give rise to transient responses of the endpoint trajectory $(x(t), y(t))$ in Fig.6, $x(t)$ and $y(t)$ in Fig.7, $q_2(t)$ and $q_4(t)$ in Fig.8 and $\dot{x}(t)$ and $\dot{y}(t)$ in Fig.9. As shown in Figs.6 and 7, the endpoint trajectories become well approximately rectilinear and do not change much for different stiffness parameters, though the speed of convergence to the target deffers considerably and dependently on k. The best choice of k in this chosen set of damping factors given in eq.(9) must be around $k = 8.0$ [N/m].

Now let us discuss how to select such a good set of damping factors as in eq.(9). If one of the tightest (smallest) diagonal matrix H_0 satisfying eq.(4) is found, then it is possible to select C in such a way that

$$C \geq 3.0H_0^{1/2} \tag{10}$$

Further, it should be noted that such a matrix H_0 can be selected as the smallest constant diagonal matrix satisfying

$$H(q) \leq H_0 \text{ for all } q \text{ such that } \|\boldsymbol{x}(q) - \boldsymbol{x}_d\| \leq r \tag{11}$$

where r denotes the eucleadian distance between the starting endpoint $\boldsymbol{x}(0)$ (= $(x(0), y(0))$ and the target $\boldsymbol{x}_d$, because according to eq.(6) the endpoint should remain inside the circle $\|\boldsymbol{x}(t) - \boldsymbol{x}_d\| \leq r$ for any $t > 0$. In the case of short-range reaching with $r = 0.1173$ [m] for a typical male adult with 1.65 [m] in height, the initial value of $H(q)$ with the posture shown in Fig.2 is evaluated as in Table 3. We evaluate a tighter bound H_0 starting from the data of $H(0)$ in Table 3 by adding each possible contribution of off-diagonal element $|H_{ij}(0)|$ to $H_{ii}(0)$ and $H_{jj}(0)$. By the same computer simulation based on Table 1 and 2, we find that such a choice of $C = 3.0H_0^{1/2}$ as numerically given in eq.(9) gives rise to

$$9.0C^{-1}H(q)C^{-1} < I_4 \tag{12}$$

during the transient process of reaching as shown in Fig.10.

4. Stability on a Manifold and Transferability

Now it is possible to show that a reference still state $(q^0, 0)$ shown by the posture F) in Fig.3 is stable on a manifold and there does not arise any unreasonable self-motion (see [35]) in the vicinity of $(q^0, 0)$ if $q(0)$ is close to q^0 and damping factors are chosen as in eq.(9). Then, it is possible to show that taking inner product between eq.(5) and $\{\dot{q} + C^{-1}kJ^{\mathrm{T}}\Delta\boldsymbol{x}\}$ yields

$$\frac{\mathrm{d}}{\mathrm{d}t}W(k;\Delta\boldsymbol{x},\dot{q}) + kh(\Delta\boldsymbol{x},\dot{q}) = -\dot{q}^{\mathrm{T}}C\dot{q} - k^2\Delta\boldsymbol{x}^{\mathrm{T}}JC^{-1}J^{\mathrm{T}}\Delta\boldsymbol{x} \tag{13}$$

where

$$h(\Delta\boldsymbol{x},\dot{q}) = \Delta\boldsymbol{x}^{\mathrm{T}}JC^{-1}\left(-\frac{1}{2}\dot{H} - S\right)\dot{q} - \Delta\boldsymbol{x}^{\mathrm{T}}\dot{J}C^{-1}H\dot{q} - \dot{q}^{\mathrm{T}}J^{\mathrm{T}}JC^{-1}H\dot{q} \tag{14}$$

and

$$W(k;\Delta\boldsymbol{x},\dot{q}) = \frac{1}{2}(\dot{q} + kC^{-1}J^{\mathrm{T}}\Delta\boldsymbol{x})^{\mathrm{T}}H(\dot{q} + kC^{-1}J^{\mathrm{T}}\Delta\boldsymbol{x}) + \frac{k}{2}\Delta\boldsymbol{x}\{2I_2 - kJC^{-1}HC^{-1}J^{\mathrm{T}}\}\Delta\boldsymbol{x} \tag{15}$$

Equation (13) can be rewritten into

$$\frac{\mathrm{d}}{\mathrm{d}t}W(k;\Delta\boldsymbol{x},\dot{q}) = -\dot{q}^{\mathrm{T}}C\dot{q} - k^2\Delta\boldsymbol{x}^{\mathrm{T}}JC^{-1}J^{\mathrm{T}}\Delta\boldsymbol{x} - kh(\Delta\boldsymbol{x},\dot{q}) \leq -\gamma W(k;\Delta\boldsymbol{x},\dot{q}) - kh(\Delta\boldsymbol{x},\dot{q}) - f(k;\Delta\boldsymbol{x},\dot{q}) \tag{16}$$

where

$$f(k;\Delta\boldsymbol{x},\dot{q}) = \dot{q}^{\mathrm{T}}\left(C - \frac{\gamma}{2}H - \frac{\gamma k}{4}H\right)\dot{q} + k\Delta\boldsymbol{x}^{\mathrm{T}}(kJC^{-1}J^{\mathrm{T}} - \gamma I_2 - \gamma JC^{-1}HC^{-1}J^{\mathrm{T}})\Delta\boldsymbol{x} \tag{17}$$

and the following inequality is used:

$$\Delta\boldsymbol{x}^{\mathrm{T}}JC^{-1}H\dot{q} \leq \Delta\boldsymbol{x}^{\mathrm{T}}JC^{-1}HC^{-1}J^{\mathrm{T}}\Delta\boldsymbol{x} + \frac{1}{4}\dot{q}^{\mathrm{T}}H\dot{q} \tag{18}$$

Now, assume that a reference still state $(q^0, 0)$ with $\boldsymbol{x}(q^0) = \boldsymbol{x}_d$ is given as shown in FIg.3 with the posture F) and choose positive numbers $\delta_1 > 0$ and $r_0 > 0$ appropriately so that any q in $N^8(\delta_1, r_0)$ satisfies eq.(11), eq.(12), and another inequality $J(q)C^{-1}J^{\mathrm{T}}(q) > 0.215I_2$. Then, it is possible to prove the following theorems:

Theorem 1 The reference state $(q^0, 0)$ is stable on a manifold for the closed-loop dynamics of eq.(5) with $k = 10.0$ and damping factors given in eq.(9).

Theorem 2 The neighborhood $N^8(\delta_1, r_1)$ with some δ_1 and r_1 such that $0 < \delta_1 < r_0$ and $0 < r_1 < r_0$ is transferable to a submanifold of M_2.

The proofs of these theorems are omitted in this paper, because they are straightforward from Theorem 3 to be stated in the next section.

5. Pointwise Transferability and Middle-range Reaching

It should be noted that both Theorem 1 and 2 can assure asymptotic convergence of endpoint trajectories $|vecx(t)$ to $\boldsymbol{x}_d$ starting from a broad domain of initial postures $q(0)$, in particular, even if the finger joint angle $q_4(0)$ differs fairly from $q_4^0(0)$, because the fourth diagonal entry $H_{44}(q)$ of $H(q)$ is quite small relative to other diagonal entries $H_{ii}(q)$ $(i = 1, 2, 3)$ owing to the smaller link inertia moment of index finger. Therefore, both the theorems do not assure non-occurence of possible self-motion of a part of the whole arm, that is, partial joint angles $(q_3(t),\ q_4(t))$ of finger joint and wrist. In order to analyze more rigorously the problem whether self-motion may arise or not, it is important to fefine the following:

Point-wise transferability For a target point $\boldsymbol{x}_d = (x_d,\ y_d)$ for the closed-loop dynamics of eq.(5), an initial still state $(q(0),\ \dot{q}(0) = 0)$ is said to be pointwise transferable to a submanifold of M_2 if and only if the endpoint $\boldsymbol{x}(t)$ $(= \boldsymbol{x}(q(t))$ of the solution $(q(t),\ \dot{q}(t))$ to eq.(5) starting from $(q(0),\ 0)$ converges $\boldsymbol{x}_d$ as $t \to \infty$ under the condition that

$$\sum_{i=1}^{4} l_i \left| q_i(t) - q_i(0) \right| \leq 2\alpha\pi \| \boldsymbol{x}(0) - \boldsymbol{x}_d \| \tag{19}$$

for any $t \geq 0$ with a constant α of $O(1)$.

Since l_i denotes the length of link i, the left hand side of eq.(19) is equivalent to the total of movements of each link endpoint relative to each corresponding joint. We interprete that if eq.(19) is valid for at most $\alpha = O(1)$ then there does not arise self-motion caused by joint redundancy.

Now we show that, given a target endpoint $\boldsymbol{x}_d$ as in Fig.3 and an initial posture as S) of Fig.3, this initial state $(q(0),\ 0)$ of the closed-loop dynamics (5) with damping factors of eq.(9) becomes pointwise transferable with $\alpha = 1.0$. As discussed in section 3, it is reasonably assumed that inequality (12) is valid for any q during this reaching movement. Furthermore, it is easy to see that the lowest eigenvalue of $J(q)C^{-1}J^{\mathrm{T}}(q)$ is always bounded from below by $\lambda_m = 0.18$ as shown in Fig.10 (a), which leads to

$$J(q)C^{-1}J^{\mathrm{T}}(q) \geq 0.18 I_2 \tag{20}$$

At the same time, it is easy to check that

$$J(q)J^{\mathrm{T}}(q) \leq (1/2)I_2 \quad \text{and} \quad C \geq (9/2)H(q) \tag{21}$$

Then, it is possible to show by putting $k = 8.0$ and $\gamma = 4/3$ the function f defined by eq.(17) can be evaluated as follows:

$$f(k = 8.0; \Delta\boldsymbol{x}, q) \geq (1/4)\dot{q}^{\mathrm{T}} C \dot{q} \tag{22}$$

On the other hand, the function h can be evaluated in a similar manner to the appendices presented in our previous paper [36] such that

$$kh(\Delta\boldsymbol{x}, \dot{q}) = 8.0h(\Delta\boldsymbol{x}, \dot{q}) \geq -(1/4)\dot{q}^{\mathrm{T}} C \dot{q} \tag{23}$$

Thus, from eqs.(22) and (23) it follows that

$$\frac{\mathrm{d}}{\mathrm{d}t} W(\Delta\boldsymbol{x}, \dot{q}) \leq -(4/3) W(\Delta\boldsymbol{x}, \dot{q}) \tag{24}$$

where $W(k; \Delta\boldsymbol{x}, \dot{q})$ at $k = 8.0$ is denoted by $W(\Delta\boldsymbol{x}, \dot{q})$. Since $W(\Delta\boldsymbol{x}, \dot{q}) \geq (3/4)k\|\Delta\boldsymbol{x}\|^2$ for $k = 8.0$ as shown in Appendix A, it is concluded from eq.(24) that

$$\|\Delta\boldsymbol{x}(t)\|^2 \leq (4/3)\|\Delta\boldsymbol{x}(0)\|^2 e^{-(4/3)t} \tag{25}$$

because $W(\Delta\boldsymbol{x}(0), \dot{q}(0) = 0) = k\|\Delta\boldsymbol{x}(0)\|^2$. Since $\dot{q}(0) = 0$ in this case, multiplying $C^{-1/2}$ from the left to eq.(5) and integrating this resultant equation over $(0, t)$ yield

$$\begin{aligned} C^{1/2}(q(t) - q(0)) &= -C^{-1/2}H(q)\dot{q}(t) \\ &+ \int_0^t C^{-1/2}\left(\frac{1}{2}\dot{H} - S\right)\dot{q}\mathrm{d}\tau - k\int_0^t C^{-1/2}J^{\mathrm{T}}\Delta\boldsymbol{x}\mathrm{d}\tau \end{aligned} \tag{26}$$

Note that the Jacobian matrix can be described as

$$J(q) = (J_1, J_2, J_3, J_4) \tag{27}$$

$$\begin{cases} J_1 = \begin{pmatrix} -y \\ x \end{pmatrix}, \qquad J_2 = \begin{pmatrix} -y + l_1 s_1 \\ x - l_1 c_1 \end{pmatrix} \\ J_3 = \begin{pmatrix} -l_1 s_{1234} - l_2 s_{123} \\ l_1 c_{1234} + l_2 c_{123} \end{pmatrix},\ J_4 = \begin{pmatrix} -l_1 s_{1234} \\ l_1 c_{1234} \end{pmatrix} \end{cases} \tag{28}$$

where s_{123} denotes $\sin(q_1 + q_2 + q_3)$, $c_{123} = \cos(q_1 + q_2 + q_3)$, etc. Hence it follows from eq.(26) that

$$\begin{aligned} \sqrt{c_i}|q_i(t) - q_i(0)| &\leq \frac{1}{\sqrt{c_i}}\left|\sum_{j=1}^{4} H_{ij}\dot{q}_i\right| \\ &+ \bar{\beta}\int_0^\infty \dot{q}^{\mathrm{T}} C \dot{q}\mathrm{d}\tau + \frac{k}{\sqrt{c_i}}\int_0^t \|J_i\|\|\Delta\boldsymbol{x}\|\mathrm{d}\tau \end{aligned} \tag{29}$$

where $\bar{\beta}$ can be evaluated as at most $\bar{\beta} = 0.2$. Comparing numerical values of c_i defined by eq.(9) and the length l_i given in Table 1, we find that $\sqrt{c_i}$ is close to $O(4l_i)$. Further, since $\boldsymbol{x}_d = (-0.35, 0.35)$, $\|\Delta\boldsymbol{x}(0)\| = 0.1173$ [m], and $\boldsymbol{x}(t)$ remains inside the circle $\|\Delta\boldsymbol{x}\| = 0.1173$, it is possible to see that $\|J_1\| \leq \|\boldsymbol{x}_d\| + \|\Delta\boldsymbol{x}(0)\| = 0.6123$, and similarly $\|J_2\| \leq 0.465$, $\|J_3\| \leq 0.185$, and $\|J_4\| \leq 0.09$. On the other hand, it is possible to obtain

$$\frac{1}{\sqrt{c_i}}\left|\sum_{j=1}^{4} H_{ij}\dot{q}_i\right| + \bar{\beta}\int_0^\infty \dot{q}C\dot{q}\mathrm{d}\tau \leq \sqrt{c_i}h_0\sqrt{E(t)} + \beta E(0) \tag{30}$$

where h_0 is at most 0.1. Thus, by using $(k/2)\|\Delta\boldsymbol{x}(0)\|^2 = E(0)$, it is possible to obtain

$$\begin{aligned} d_i = l_i\|q_i(t) - q_i(0)\| \leq 2\left(l_i h_0 + \frac{l_i}{\sqrt{c_i}}\bar{\beta}\sqrt{E(0)}\right)\|\Delta\boldsymbol{x}(0)\| \\ + \frac{16}{c_i\sqrt{3}} l_i \left\{ int_0^t \|J_i\| e^{-(2/3)\tau}\mathrm{d}\tau \right\}\|\Delta\boldsymbol{x}(0)\| \end{aligned} \tag{31}$$

The second term of the right hand side is dominant relative to the first. In fact, the first term of the right hand side

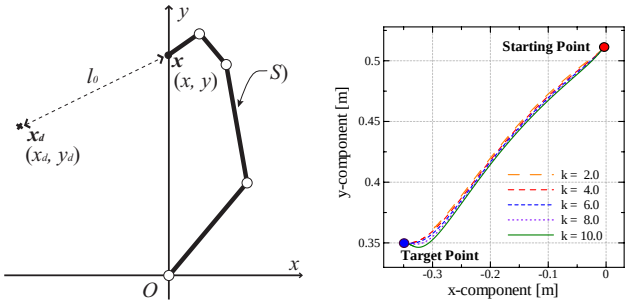

(a) (b)

Figure 11: (a) Starting position, where $l_0 = \|\boldsymbol{x} - \boldsymbol{x}_d\| = 0.3823$ [m]. (b) Transient responses of the endpoint in case of middle-range reaching with the same set of damping factors as given in eq.(9).

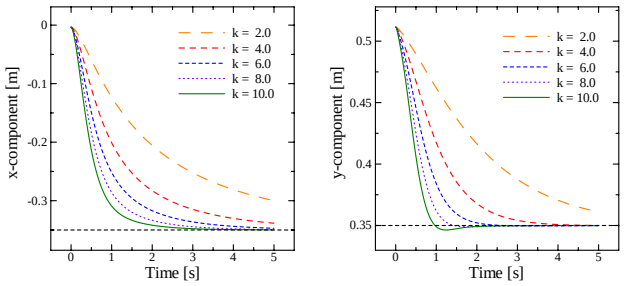

(a) (b)

Figure 12: Transient responses of $x(t)$ and $y(t)$ corresponding to the case of Fig.11.

Table 4: Initial conditions.

$q_1(0)$	50.00	[deg]
$q_2(0)$	50.00	[deg]
$q_3(0)$	30.00	[deg]
$q_4(0)$	85.00	[deg]
$x(0)$	-0.003429	[m]
$y(0)$	0.5114	[m]
$\|\Delta\boldsymbol{x}\|_2$	0.3823	[m]

is bounded from above by a quantity $\varepsilon_0\|\Delta\boldsymbol{x}(0)\|$ with $\varepsilon_0 = 0.08$. Thus, we obtain

$$\begin{cases} d_1 \le (\varepsilon_0 + 1.257)\|\Delta\boldsymbol{x}(0)\|, & d_2 \le (\varepsilon_0 + 1.491)\|\Delta\boldsymbol{x}(0)\| \\ d_3 \le (\varepsilon_0 + 0.840)\|\Delta\boldsymbol{x}(0)\|, & d_4 \le (\varepsilon_0 + 1.604)\|\Delta\boldsymbol{x}(0)\| \end{cases}$$

which verifies inequality (19) with $\alpha = (4\varepsilon_0 + 5.192)/2\pi < 1.0$. This proves the following:

Theorem 3 For a given taraget point $\boldsymbol{x}_d = (x_d, y_d)$ as specified in Fig.2 or Fig.3 with $x_d = -0.35$ and $y_d = 0.35$ [m], the initial still state $(q(0), 0)$ with posture S) of Fig.3 is pointwise transferable to a submanifold of M_2 without self-motion.

Not only in the case of short-range reaching discussed above but also in the case of middle-range reaching such as $\|\Delta\boldsymbol{x}(0)\| = 0.3823$ [m] (see Fig.11 (a)) and the initial posture and endpoint are given in details as in Table 4, the endpoint trajectories of solutions to the closed-loop dynamics of eq.(5) with the same damping factors of eq.(9) for various values of stiffness parameter k converge to $\boldsymbol{x}_d$ as shown in Fig.11 (b). In this case the transient responses of $x(t)$ and $y(t)$ become as shown in Fig.12. It is interesting to see that the speed of convergence to the target shown in Fig.12 is not so retarded in comparison with that of the previous short-range reaching case shown in Fig.7, regardless that the initial distance to the target $\|\Delta\boldsymbol{x}(0)\| = 0.3823$ [m] in the middle-range reaching is more than three times of the initial distance $\|\Delta\boldsymbol{x}(0)\| = 0.1173$ [m] in the short-range case. However, it seems not so easy to prove the pointwise transferability without self-motion in this middle-range reaching, because the minimum eigenvalue of $J(q)C^{-1}J^{\mathrm{T}}(q)$ may happen to become smaller below $\lambda_m = 0.18$. Notwithstanding this, it is possible to conclude the statement of Theorem 3 for the middle-range reaching by using the argument developed in section 7.

6. Virtual-spring Hypothesis and Typical Characteristics of Skilled Reaching Movements

The analysis of closed-loop dynamics of eq.(6) developed in previous sections suggests that, to realize a skilled reaching motion by using redundant joints, generation of an artificial potential $(k/2)\|\Delta\boldsymbol{x}\|^2$ together with an adequate set of damping factors is not only indispensable but also sufficient for generating a quasi-straight line movement of the endpoint. In the case of control of a robotic arm, the term $-kJ^{\mathrm{T}}(q)\Delta\boldsymbol{x}$ is called a task-space feedback based on measurements of the endpoint position $\boldsymbol{x}(t)$ by external sensing like visual sensing. In the case of human reaching, however, exerted torques $-kJ^{\mathrm{T}}(q)\Delta\boldsymbol{x}$ must be generated from a group of muscles which are endowed with a total potential energy generated by excitation of neuro-motor signals from the CNS. This fact can be well interpreted by hypothesizing a virtual spring as shown in Fig.13, drawing the end of the whole arm to the target with the force equivalent to the vector $k(\boldsymbol{x}_d - \boldsymbol{x}(t))$, which is equivalent to $-k\Delta\boldsymbol{x}$. In this hypothesized model, the ith joint is exerted by the torque $-kJ_i^{\mathrm{T}}\Delta\boldsymbol{x}$ and also subject to the damping force $-c_i\dot{q}_i$. It should be remarked that the magnitude and signature of each spring-like moment of force at each joint are not directly related to the magnitude of $\Delta\boldsymbol{x}$ but to the quantity of k times an inner product of two-dimensional vectors $J_i(q)$ and $\Delta\boldsymbol{x}$, where $J_i(q)$ $(i = 1, \cdots, 4)$ are defined in eq.(28). Note that the magnitude of $-kJ_i^{\mathrm{T}}\Delta\boldsymbol{x}$ is equivalent to that of moment of force $\overrightarrow{P_iP_0} \times k\Delta\boldsymbol{x}$, where symbol "$\times$" denotes

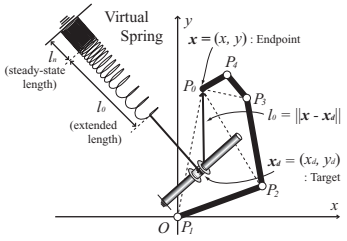

Figure 13: Virtual-Spring Hypothesis

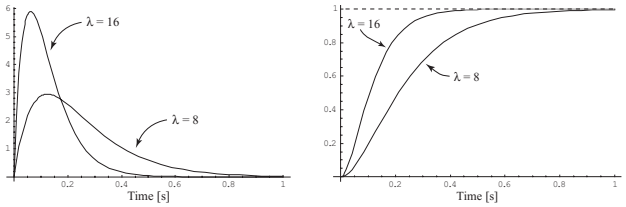

(a) $\lambda^2 te^{-\lambda t}$ (b) $1 - e^{-\lambda t} - \lambda te^{-\lambda t}$

Figure 15: Time-varying stiffness parameter.

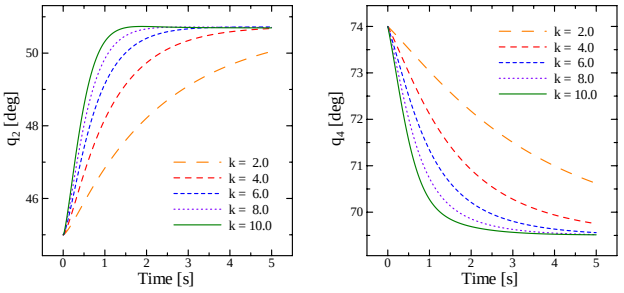

(a) $q_2(t)$ (b) $q_4(t)$

Figure 14: Transient responses of joint angles q_2 and q_4 when damping factors of eq.(32) are chosen.

the external product and $\overrightarrow{P_iP_0}$ denotes the position vector from the ith joint to the endpoint (see Fig.13). Therefore, in the case of short-range reaching starting from the posture S) in Fig.3 (b) the torque $-kJ_1^{\mathrm{T}}\Delta\boldsymbol{x}$ exerting to the shoulder joint is plus at $t = 0$ and therefore $q_1(t)$ is increasing with t as well as $q_2(t)$ seen in Fig.8 (a), but the torque $-kJ_4^{\mathrm{T}}\Delta\boldsymbol{x}$ exerting to the finger joint is minus at $t = 0$ and therefore $q_4(t)$ is decreasing with t as seen in Fig.8 (b). On the basis of this virtual-spring hypothesis, it can be claimed that a skilled reaching movement must emerge from synergistic generations of potential energies in a group of muscles involved in these four joints, whose total is equivalent to $(1/2)k\|\Delta\boldsymbol{x}(0)\|^2$, and synergistic formation of damping factors generating viscouse-like forces in each subgroup of muscles corresponding to each joint. Variability of joint motions is mainly due to permissible fluctuations of damping effects, which are rather insensitive to the endpoint trajectory. Thus, the fourth characteristics of human skilled reaching raised as d) in section 3 become apparent from the viewpoint of virtual-spring hypothesis. Each joint movement is fairly dependent on the posture and in details subject to exertion of each corresponding torque $-kJ_i^{\mathrm{T}}(q)\Delta\boldsymbol{x}$.

Next, we discuss the variability as the most reproducable characterisitcs of human multi-joint reaching. Let us choose another set of damping factors:

$$c_1 = c_2 = 1.89, \qquad c_3 = c_4 = 0.29 \quad [\mathrm{Nms}] \qquad (32)$$

Compared with the previous set of damping factors of eq.(9), this choice of dampings means that exertion of damping forces on the finger MP joint and elbow is enhanced considerably relative to the wrist and shoulder respectively. Note that both the wrist and shoulder are a universal joint but the finger MP joint and elbow are not. Computer simulation based on the closed-loop dynamics of eq.(5) by using damping factors of eq.(32) gives rise to almost the same quasi-straight line endpoint trajectory $\boldsymbol{x}(t)$ as in Fig.6. Notwithstanding this, movements of joints are noticeably variable according to changes of their corresponding damping factors as shown in Fig.14 in comparison with Fig.8. In fact, note that the index finger MP joint rotates from 74 [degree] to about 63.0 [degree] in Fig.8 but it does from 74 [degree] to about 69.0 [degree] in Fig.14, and the elbow rotates from 45 [degree] to about 52.7 [degree] but it does to 50.7 [degree] in Fig.14 (a). That is, each joint motion is quite sensitive to change of its corresponding damping factor but the profile of endpoint trajectory is not so variable in a wide range in the set of damping factors c_i $(i = 1, \cdots, 4)$.

Finally, another two typical characteristics of human skilled reaching as described b) and c) in section 3 must be discussed more in detail. In case of human multi-joint movements, each joint is not directly actuated but rotated indirectly by contraction of a group of muscles involved in each corresponding joint. Muscle contraction can be interpreted from the mechanics viewpoint as a cause of generation of a potential energy produced from chemical reactions stimulated by pulse-modulated neuro-motor signals conveyed from the CNS. As it is now well known [37] ~ [39], an elementary process of force generation during muscle contraction is based on movements of a head of myosin motor protein along an action filament triggered by pivoting of the lever arm as a part of myosin light-chain domain [40]. If this actomyosin (mechano-chemical interaction between nyosin molecules and actin-filaments) is treated as a stochastic process of force generation and thereby a population of these actomyosin activities are subject to a typical gamma distribution with a density function in time as $p(t) = \lambda^2 te^{-\lambda t}$ with a parameter $\lambda > 0$ (see Fig.15 (a)), then generation of the total potential produced by contractions of the whole muscles must be time-varying with an approximate stiffness parameter proportional to the integral

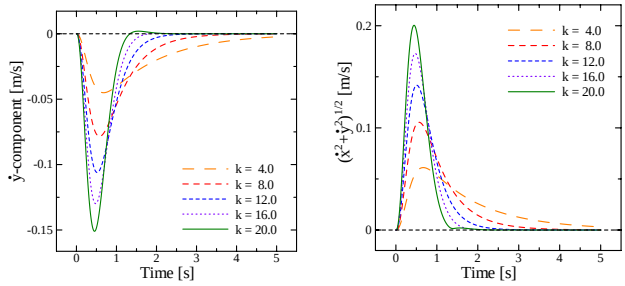

(a) (b)

Figure 16: Transient responses of $\dot{y}(t)$ and $v = \sqrt{\dot{x}^2(t) + \dot{y}^2(t)}$ corresponding to the case of Fig.3(a) where $c_1 = 2.67$, $c_2 = 1.71$, $c_3 = 0.410$, $c_4 = 0.0990$ [Ns].

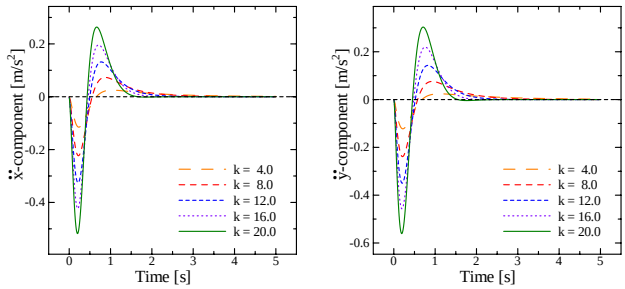

(a) (b)

Figure 17: Transient responses of $\ddot{x}(t)$ and $\ddot{y}(t)$ corresponding to the case of Fig.3(a) where $c_1 = 2.67$, $c_2 = 1.71$, $c_3 = 0.410$, $c_4 = 0.0990$ [Ns].

of $p(t)$, i.e.,

$$k(t) = k_0 \int_0^t p(\tau)\mathrm{d}\tau \tag{33}$$

Thus, it can be interpreted that a total of whole chemical reactions leads to time-varying generation of a total potential energy in such a function form as

$$\frac{1}{2}k(t)\|\Delta\boldsymbol{x}(t)\|^2$$

and $k(t)$ is a monotonously increasing function in t as shown in Fig.15.

Figures 16 and 17 show computer simulation results concerning the closed-loop dynamics

$$H(q)\ddot{q} + \left(\frac{1}{2}\dot{H}(q) + S(q,\dot{q})\right)\dot{q} + C\dot{q} + k(t)J^{\mathrm{T}}(q)\Delta\boldsymbol{x} = 0 \tag{34}$$

which follows from substituting the control signal

$$u = -C\dot{q} - k(t)J^{\mathrm{T}}(q)\Delta\boldsymbol{x} \tag{35}$$

into eq.(3), where $k(t)$ is defined by eq.(33) with stiffness constant k_0. In this simulation, we set $\lambda = 8.0$ and double

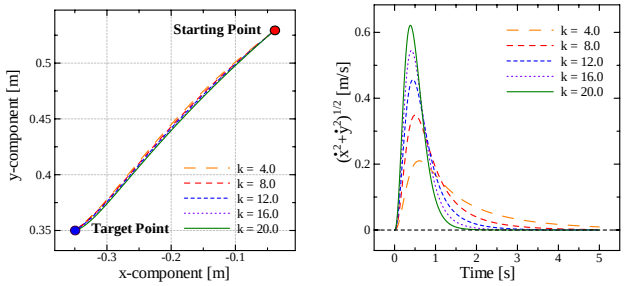

(a) (b)

Figure 18: Transient responses of the endpoint and $\sqrt{\dot{x}^2(t) + \dot{y}^2(t)}$ corresponding to the case of $c_1 = 2.67$, $c_2 = 1.71$, $c_3 = 0.141$, $c_4 = 0.0354$ [Ns] and the initial posture of Table 5.

Table 5: Initial conditions.

$q_1(0)$	59.00	[deg]
$q_2(0)$	43.00	[deg]
$q_3(0)$	25.00	[deg]
$q_4(0)$	95.00	[deg]
$x(0)$	-0.03806	[m]
$y(0)$	0.5295	[m]
$\|\|\Delta\boldsymbol{x}\|\|$	0.3599	[m]

each k in the previous simulation (Figs.6 to 10) in such a way as $k_0 = 2k$. Accordingly, each c_i in Fig.9 is multiplied by $\sqrt{2}$ so that the joint motion $q(t)$ in eq.(6) can be accelerated by setting $k = \kappa k_0$ and $c_i = \sqrt{\kappa}c_{0i}$ $(i = 1, \cdots, 4)$ with a positive parameter $\kappa > 0$. In fact, if $q(t)$ is a solution to eq.(9) for a stiffness parameter $k = k_0$ and a set of damping factors $c_i = c_{0i}$ $(i = 1, \cdots, 4)$, then $q(\kappa t)$ must be the solution to eq.(9) for $k = \kappa k_0$ and $c_i = \sqrt{\kappa}c_{0i}$ under the same initial condition that $q(0) = q^0$ and $\dot{q}(0) = 0$. As seen in Fig.16, velocity profiles of $\dot{y}(t)$ and v $(= \sqrt{\dot{x}^2 + \dot{y}^2})$ become bell-shaped, and in particular the profile of $\dot{y}$ in Fig.16 (a) becomes more symmetric campared with Fig.9 (b). It should be remarked again that the endpoint trajectories $(x(t), y(t))$ become a quasi-straight line and behave almost the same as Fig.6. It is interesting to note that transient responses of accelerations $\ddot{x}$ and $\ddot{y}$ have double peaks as seen in Fig.17, which is coincident with the third characteristics c) of human skilled reaching.

Finally we show in Fig.18 results of a simulation in the case of middle-range reaching starting from the initial posture shown in Table 5. Compared with Fig.11 (b), the endpoint trajectory of Fig.18 (a) becomes more straight and the velocity profile of Fig.18 (b) becomes more symmetirc. In this case, note that the rate of damping coefficients c_3 and c_4 per c_1 and c_2 respectively is reduced considerably. In other words, softening both finger and wrist joints relative

to elbow and shoulder joints makes the endpoint movement direct more straightforwardly to the target throughout the whole motion.

7. Feedforward Control and Global Reaching Movements

The virtual-spring hypothesis not only supports but also enhance the EP-hypothesis in a sense that a potential energy source (a virtual-spring) is supposed to virtually exist at the target equilibrium point and thereby a corresponding force $-k(t)\Delta\boldsymbol{x}$ that supposedly draws the endpoint of the whole arm evokes each moment of force $-k(t)J_i^{\mathrm{T}}(q)\Delta\boldsymbol{x}$ at each corresponding joint i. In other words, synergy for coordinating generations of joint torques must evolve through thousands of practices so as to emanate neuromotor signals from the CNS to activate a group of muscles to generate a total of potential $(k(t)/2)\|\Delta\boldsymbol{x}\|^2$ and individual joint damping forces. Based on the virtual-spring hypothesis, it is needless to suppose individual spring-like forces at each joint, but supposition of a single stiffness parameter $k(t)$ plays a crucial role. Therefore, as claimed by Won and Hogan [30], estimating stiffness parameters at each joint is a needless detail. Rather, it is more important to suppose that the single stiffness parameter $k(t)$ is determined in a time-varying manner so that moments of forces $-k(t)J_i^{\mathrm{T}}(q)\Delta\boldsymbol{x}$ at joint i $(i = 1, \cdots, 4)$ are produced in a feedforward manner. In other words, the control scheme of eq.(35) may work as an open-loop feedforward control in the case of human multi-joint reaching movements. Although this paper does not take into consideration muscle dynamics, the damping force terms $-c_i\dot{q}_i$ $(i = 1, \cdots, 4)$ are also generated in a feedforward manner due to passive viscousity as one of mehcano-chemical properties of muscle structures and, in parallel, rate of the torque-velocity relation that can be also regulated by neuro-motor signals from the CNS [41]. It should be also pointed out that change of mechanical impedance centering at such a viscous-like term must be played by coactivitation of antagonist muscles [42]. Enhancement of the feedback gain from spinal reflex loop by co-contraction of an antagonist pair of muscles is pointed out [43], which may result in increasing the viscosity in joints.

It is interesting to note that there is no feedback loop in control signals of eq.(35). This comes from limitation of the present analysis to the case that movements of the whole arm are confined to a horizontal plane. Motion of the arm in a vertical plane needs regulation for withstanding the gravity force, that may be subject to a feedback loop from the spinal reflex, too.

A mathematical proof for verifying the pointwise transferability without incurring self-motion in the case of middle-range reaching with time-varying stiffness $k(t)$ would be more sophisticated. In this paper, only a rough sketch of the proof is given. First, analysis of the equation of motion is split into two cases of time intervals $I_1 = [0, T)$ and $I_2 = [T, \infty)$, where T must be chosen approximately as an instant when the endpoint enters into a circle with center $\boldsymbol{x}_d$ and radius r_0 with $O(10^{-1})$ [m], that is, in a circle with short-range reaching, and at the same time $k(t)$ becomes almost constant, that is, the time rate of $k(t)$ $(\dot{k}(t))$ becomes sufficiently small. In the case of an initial posture shown in Fig.11 (a), it is possible to see that $J_4^{\mathrm{T}}(q)\Delta\boldsymbol{x} < 0$ but all others $J_i^{\mathrm{T}}(q)\Delta\boldsymbol{x} > 0$ $(i = 1, 2, 3)$. This means that at the beginning of joint movements the ith joint for $i = 1, 2, 3$ rotates in the positive direction (counter-clockwise) and the fourth joint rotates in the negative direction. If the damping factors c_i $(i = 1, \cdots, 4)$ are carefully chosen as in eq.(9) or in Fig.18 and all the joints keep to rotate in their same directions as those at $t = 0$ until the time $T > 0$ specified above, that is, the endpoint has already reached inside the circle with center $\boldsymbol{x}_d$ and radius r_0 of $O(10^{-1})$ [m] at T, then the rigorous proof for short-range reaching can be applied to the latter stage of joint movements for the time interval $[T, \infty)$.

Finally, it is important to introduce the property:

Stable Transferability For a given target $\boldsymbol{x}_d = (x_d, y_d)$ for the closed-loop dynamics of eq.(6), an initial still state $(q(0), 0)$ is said to be stably transferable to a submanifold of M_2 if 1) it is pointwise transferable without self-motion to a submanifold of M_2 and 2) for an arbitrary given $\varepsilon > 0$ there exists a $\delta(\varepsilon) > 0$ such that any solution $(\bar{q}(t)\dot{\bar{q}}(t))$ starting from an arbitrary still state $(\bar{q}(0), 0)$ satisfying $\|\bar{q}(0) - q(0)\| < \delta(\varepsilon)$ is also pointwise transferable without self-motion and its final posture $\bar{q}_\infty$ $(= \lim_{t\to\infty} \bar{q}(t))$ satisfies $\|\bar{q}_\infty - q_\infty\| \leq \varepsilon$, where $q_\infty = \lim_{t\to\infty} q(t)$.

This property should be satisfied as a matter of course in human multi-joint reaching because if a given pre-shaped initial still state is stably transferable then there does not arise any oscillatory or chaotic self-motion in reaching movements starting from any still state in the vicinity of the concerned pre-shaped posture. However, a rigorus mathematical analysis for proving this property is rather difficult, though the property is valid for most cases according to computer simulations regarding robotic arms and numerous observations on human limb motions.

8. Conclusion

This paper challenges Bernstein's Degrees-of-Freedom problem in the case of redundant multi-joint reaching movements. By enhancing the EP-hypothesis for generation of reaching motions under the situation of excess joints, the virtual-spring hypothesis is proposed, which gives rise to the simplest structure of control signals without solving any inverse kinematics and dynamics problems. The control signal is composed of a term of task-space position feedback with a single stiffness parameter considered to evoke from the potential energy that the virtual-spring retains and another damping term with different but synergistic coefficients of damping at each joint. Regard-

less of redundancy of joints, this simplest control results in exhibiting typical characteristics of human-like skilled motion such as a) invariance of the special shape of endpoint trajectories, b) bell-shaped profiles of endpoint velocity signals, c) double peaks of endpoint accelerations, and d) noteworthy variability in each joint movement every trial by trial. It is also discussed by referring to recent discoveries on mechano-chemical behaviours of molecular motors that the task-space position feedback must be generated in a feedforward manner in case of human limb motions.

References

[1] N.A. Bernstein (M.L. Latash translated from the Russian by M.L. Latash), *On Dexterity and Its Development*, Lawrence Erlbaum Associates, Inc. (1996).

[2] N.A. Bernstein, *The Coordination and Regulation of Movements*, Pergamon, London (1967).

[3] J. Lenarcic (ed.), *Special Issue on Redundant Robots. Laboratory Robotics and Automation*, **6**–1 (1991).

[4] Y. Nakamura, *Advanced Robotics: Redundancy and Optimization*, Addison-Wesley, Reading, MA (1991).

[5] O. Khatib, A unified approach for motion and force control of robot manipulators: The operational space formulation, *IEEE J. Robotics and Automation*, **RA–3**, 43–53 (1987).

[6] J.M. Hollerbach and K.C. Suh, Redundancy resolution of manipulators through torque optimization, *IEEE J. of Robotics and Automation*, **RA–3**, 308–316 (1987).

[7] T. Yoshikawa, Manipulability of robotic mechanisms, *Int. J. Robotics Res.*, **4**, 3–9 (1984).

[8] V. Potkonjak, S. Tzafestas, D. Kostic, G. Djoudjevic, and M. Rasic, The handwriting problem, *IEEE Robotics & Automation Magazine*, March 2003, 35–46 (2003).

[9] Y. Nakamura and H. Hanafusa, Task priority based redundancy control of robot manipulators, in H. Hanafusa & H. Inoue (eds.), *Robotics Research: The Second Int. Symp.*, MIT Press, Cambridge, MA, pp. 447–456 (1985).

[10] J. Baillieul, Avoiding obstacles and resolving kinematic redundancy, *Proc. of the IEEE Int. Conf. on Robotics and Automation*, San Francisco, CA, pp. 1698–1704 (1986).

[11] D.E. Whitney, Resolved motion rate control of manipulators and human protheses, *IEEE Trans. Man-Machine Syst.*, **MMS–10**, 47–53 (1969).

[12] A. Liegeois, Automatic supervisory control of the configuration and behavior of multi-body mechanism, *IEEE Trans. Systems, Man, and Cybern.*, **SMC–7**, 868–871 (1977).

[13] A.G. Feldman, Once more on the equilibrium-point hypothesis (λ model) for motor control, *J. Mot. Behav.*, **18**, 17–54 (1986).

[14] T. Flash, The control of hand equilibrium trajectories in multi-joint arm movements, *Biological Cybernetics*, **57**, 257–274 (1987).

[15] T. Flash and N. Hogan, The coordination of arm movements: An experimentally confirmed mathematical model, *J. Neurosci.*, **5**, 1688–1703 (1985).

[16] A.P. Georgopoulos, On reaching, *Ann Rev. Neurosci.*, **9**, 147–170 (1986).

[17] E. Bizzi, N. Hogan, F.A. Mussa-Ivaldi, S. Giszter, Does the nervous system use equilbrium-point control to guide single and multiple joint movements?, *Behav. Brain Sci.*, **15**, 603–613 (1992).

[18] A.G. Feldman, Functional tuning of the nervous system with control of movement or maintenance of steady posture. III. Mechanographic analysis of the execution by man of the simplest robot tasks, *Biophysics*, **11**, 766–775 (1966).

[19] E. Bizzi, A. Polit, and P. Morasso, Mechanisms underlying achievement of final head position, *J. Neurophysical*, **39**, 435–444 (1976).

[20] S. Arimoto, Intelligent control of multi-fingered hands, *Annual Review in Control*, **28**-1, 75–85 (2004).

[21] N. Hogan, An organizing principle for a class of volundary movements, *J. Neurosci.*, **4**, 2745–2754 (1984).

[22] W. Nelson, Physical principle for economies of skilled movements, *Biol. Cybern.*, **46**, 135–147 (1983).

[23] Z. Hasan, Optimized movement trajectories and joint stiffness in unperturbed, initially loaded movements, *Biol. Cybern.*, **53**, 373–382 (1986).

[24] Y. Uno, M. Kawato, and R. Suzuki, Formation and control of optimal trajectory in human multijoint arm movement, *Biol. Cybern.*, **61**, 89–101 (1989).

[25] M. Kawato, Y. Maeda, Y. Uno, and R. Suzuki, Trajectory formation of arm movemnent by cascade neural network model based on minimum torque-change criterion, *Biol. Cybern.*, **62**, 275–288 (1990).

[26] H. Cruse, E. Wischmeyer, M. Bruwer, P. Brockfield, and A. Dress, On the cost function for the control of the human arm movement, *Biol. Cybern.*, **62**, 519–528 (1990).

[27] M. Takegaki and S. Arimoto, A new feedback method for dynamic control of manipulators, *Trans. of the ASME, Journal of Dynamic Systems, Measurement, and Control*, **103**-2, 119–125 (1981).

[28] S. Arimoto, H. Hashiguchi, and R. Ozawa, A simple control method coping with a kinematically ill-posed inverse problem of redundant robots: analysis in case of a handwriting robot, *Asian J. of Control*, **7**-2, (2004).

[29] S. Arimoto, Intelligent control of multi-fingered hands, *Annual Review in Control*, **28**, 75–85 (2004).

[30] J. Won and N. Hogan, Stability properties of human reaching movements, *Exp. Brain Res.*, **107**, 125–136 (1995).

[31] D.J. Bennett et al., Time-varying stiffness of the human elbow joint during cyclic voluntary movement, *Exp. Brain Res.*, **88**, 433–442 (1992).

[32] H. Gomi and M. Kawato, Equilibrium-Point hypothesis examined by measured arm stiffness during multijoint movement, *Science*, **272**, 117–120 (1996).

[33] M.L. Latash, *Neurophysiological Basis of Movement*, Human Kinetics Pub., New York (1998).

[34] S. Arimoto, *Control Theory of Nonlinear Mechanical Systems: A Passivity-based and Circuit-theoretic Approach*, Oxford Univ. Press, Oxford, UK (1996).

[35] H. Seraji, Configuration control of redundant manipulators: Theory and implementation, *IEEE Trans. on Robotics and Automation*, **5**-4, 472–490 (1989).

[36] S. Arimoto, M. Sekimoto, H. Hashiguchi, and R. Ozawa, Natural resolution of ill-posedness of inverse kinematics for redundant robots: A challenge to Bernstein's degrees-of-freedom problem, to be published in *Advanced Robotics*, **19**, (2005).

[37] T. Yanagida, T. Arata, and F. Oosawa, Sliding distance of actin filament induced by a myosin crossbridge during one ATP hydrolysis cycle, *Nature*, **316**, 366–369 (1985).

[38] J.A. Spudich, How molecular motors work, *Nature*, **372**, 515–518 (1994).

[39] R.D. Vale and R.A. Milligan, The way things move: looking under the hood of molecular motor proteins, *Science*, **288**, 88–95 (2000).

[40] K. Kitamura, M. Tokunaga, A.H. Iwane, and T. Yanagida, A single myosin head moves along an action filament with regular steps of 5.3 nanometers, *Nature*, **397**, 129–134 (1999).

[41] J.M. Winters and L. Stark, Muscle models: What is gained and what is lost by varying model complexity, *Biol. Cybern.*, **55**, 403–420 (1987).

[42] N. Hogan, The mechanics of multi-joint posture and movement control, *Biol. Cybern.*, **52**, 315–331 (1985).

[43] P.L. Gribble, L.I. Mullin, et al., Role of cocontraction in arm movement accuracy, *J. of Neurophysiology*, **89**, 2396–2405 (2003).

Appendix A

By using the inequality

$$k\dot{q}^{\mathrm{T}}HC^{-1}J^{\mathrm{T}}\Delta\boldsymbol{x} \geq -\frac{1}{2}\dot{q}^{\mathrm{T}}H\dot{q} - \frac{k^2}{2}\Delta\boldsymbol{x}^{\mathrm{T}}JC^{-1}HC^{-1}J^{\mathrm{T}}\Delta\boldsymbol{x}$$

and noting $J(q)J^{\mathrm{T}}(q) \leq 0.5I_2$, it is easy to check that, when $k = 8.0$,

$$\begin{aligned} W(k;\Delta\boldsymbol{x},\dot{q}) = {} & \frac{1}{2}\dot{q}^{\mathrm{T}}H(q)\dot{q} + k\|\Delta\boldsymbol{x}\|^2 + k\dot{q}^{\mathrm{T}}H(q)C^{-1}J^{\mathrm{T}}(q)\Delta\boldsymbol{x} \\ \geq {} & k\|\Delta\boldsymbol{x}\|^2 - (k^2/18)\Delta\boldsymbol{x}^{\mathrm{T}}J(q)J^{\mathrm{T}}(q)\Delta\boldsymbol{x} \\ \geq {} & k\left(1 - \frac{k}{18}\times\frac{1}{2}\right)\|\Delta\boldsymbol{x}\|^2 \geq \frac{3}{4}k\|\Delta\boldsymbol{x}\|^2 \end{aligned}$$